

PREPARED FOR SUBMISSION TO JHEP

Thermal regularization of t -channel singularities in cosmology and particle physics: the general case

Michał Iglicki

*Faculty of Physics, University of Warsaw,
ul. Pasteura 5, 02-093 Warsaw, Poland*

E-mail: michal.iglicki@fuw.edu.pl

ABSTRACT: This paper presents a way to regularize the t -channel singularity (which appears when a massive, stable t -channel mediator of a given process is allowed to be on-shell, making the cross section infinite) in a general case of particles of any spin $(0, 1/2, 1)$ interacting within a thermal medium. Those interactions result in a finite lifetime of the mediator and allow to introduce an effective momentum- and temperature-dependent width. As a result, the would-be-singular cross section becomes finite. A complete derivation and an analytical result for the width are provided. For an illustration, the method is used to calculate the thermal widths and cross sections within the Vector-Fermion Dark Matter model.

KEYWORDS: t -channel singularity, dark matter, thermal field theory

ARXIV EPRINT: [2212.00561](https://arxiv.org/abs/2212.00561)

Contents

| | | |
|----------|--|-----------|
| 1 | Introduction | 1 |
| 1.1 | t -channel singularity and its relevance | 1 |
| 1.2 | Known approaches | 2 |
| 1.3 | This paper | 4 |
| 2 | Dyson resummation. Effective width in terms of the particle's self-energy | 4 |
| 2.1 | Scalar state | 5 |
| 2.1.1 | Thermal tree-level propagator vs. the zero-temperature formula | 6 |
| 2.2 | Fermion state | 6 |
| 2.3 | Vector state | 7 |
| 2.4 | Effective width | 8 |
| 3 | Calculation of the regulator $\Sigma(p, T)$ | 9 |
| 3.1 | Result discussion | 14 |
| 4 | Values of the factor X_0 calculated within the VFDM model | 15 |
| 5 | Summary | 20 |
| A | Conventions | 20 |
| B | Green's functions | 21 |
| C | Allowed range of $E_{1,2}$ | 22 |
| D | Calculation of X_0 in the general case | 24 |
| E | Calculation of X_0 within the VFDM model | 26 |
| F | Results of Weldon's paper | 27 |

1 Introduction

1.1 t -channel singularity and its relevance

A t -channel singularity of a given scattering process with a t -channel mediator arises when the mediator is kinematically allowed to be on its mass-shell. Then, the mediator's propagator becomes singular. For a massive mediator, one cannot use the infrared regularization schemes. If, in addition, the mediator is stable, the usual Breit-Wigner approach cannot

be applied to regularize the singularity using the mediator’s width. This leads to a truly singular (infinite) cross section.

Examples of Standard Model processes affected by the singularity include the weak analogue of the Compton scattering, $Ze^- \rightarrow e^-Z$, mediated by electron neutrino, and neutrino-mediated muon-muon scattering, $\mu^+\mu^- \rightarrow W^+W^{*-} \rightarrow W^+e^-\bar{\nu}_e$. However, the most natural context in which the t -channel singularity appears are models of dark matter, as they provide massive stable particles that can serve as singular mediators.

It should be stressed that the t -channel singularity is a serious issue whose role cannot be reduced to some kind of higher-order corrections to nevertheless finite results. Under certain circumstances, the discussed singularity makes cross sections truly infinite. Therefore, an applicable and practical solution to this problem should be desired.

1.2 Known approaches

The existence of processes with a t -channel mediator kinematically allowed to be on-shell is known at least since early ’60s [1]. In 1965, Coleman and Norton [2] proved that *a Feynman amplitude has singularities on the physical boundary if and only if the relevant Feynman diagram can be interpreted as a picture of an energy- and momentum-conserving process occurring in space-time, with all internal particles real, on the mass shell, and moving forward in time*, which in the case of a $2 \rightarrow 2$ t -channel process is actually equivalent to the condition (1.1) formulated here. Since then, however, the topic has not been widely explored by particle physicists apart of a few papers (see, e.g., [3]).

Dating from the ’90s, several studies [4–9] concerning the t -channel singular process of $\mu^+\mu^- \rightarrow W^+e^-\bar{\nu}_e$ appeared due to its relevance for planned lepton colliders. The authors mainly proposed to cure the singularity by including corrections resulting from a finite size of the scattering beams. None of their proposals, however, is simultaneously fully reliable and applicable in the case of singular processes in the early Universe, when no beams are involved so there is no scale to be used as a regulator.

A similar mechanism has been introduced in [10] and further developed in [11]. The authors encountered the problem of t -channel singularity while considering neutrino oscillations. They propose to regularize the singularity by taking into account non-locality of interactions within the source and the detector. Although promising, that approach cannot be applied to the case this paper focuses on, for the reasons similar to those mentioned above.

Another natural idea is to include thermal corrections to the masses of the particles involved in the process, hoping that the singularity disappears, as it happens with the IR singularities in the HTL approach [12]. Unfortunately, for a massive mediator, this would only shift the singular value of momentum squared from the bare to the thermal mass squared. This could regularize the singularity only if the masses change dramatically, so that the decomposition corresponding to condition (1.1) is no longer possible.

On the other hand, for cosmological applications, a quite different method has been developed by the authors of [13] inspired by [14, 15]. Their method bases on carefully taking into account the statistical factors present in the Boltzmann equation term corresponding to the singular process. Note that in his paper [14], Weldon obtained a result similar to

eq. (3.23), working in the imaginary-time (Matsubara) formalism. His result agrees with the one presented in this paper, calculated within the real-time approach, but differs by a numerical factor, see appendix F.

In a recent publication [16] it is shown that for a $2 \rightarrow 2$ t -channel diagram, for a given set of particles' masses (two in the initial state, two in the final state, and the mediator's mass), it is possible to determine the range of the CM energy, $\sqrt{s}_1 < \sqrt{s} < \sqrt{s}_2$, that leads to appearance of the singularity. To calculate the thermally averaged cross section, used in cosmological considerations involving Boltzmann equations, one integrates over the CM energy from \sqrt{s}_{\min} (equal to the minimum possible energy of the process, i.e., sum of the initial-state masses or sum of the final-state masses, whichever is greater) to infinity. Hence, the thermally averaged cross section becomes singular whenever the singular range (\sqrt{s}_1, \sqrt{s}_2) intersects with $(\sqrt{s}_{\min}, \infty)$, i.e., whenever $\sqrt{s}_{\min} < \sqrt{s}_2$. In the case of a $2 \rightarrow 2$ process, it happens when the following conditions are simultaneously satisfied:

$$\begin{aligned}
 &\text{one of the initial-state particles can decay into} \\
 &\text{the mediator and the corresponding final-state particle} \\
 &\text{and} \\
 &\text{one of the final-state particles can decay into} \\
 &\text{the mediator and the corresponding initial-state particle,}
 \end{aligned} \tag{1.1}$$

where by the „corresponding particle” one should understand the particle connected by the same vertex to the decaying particle and the mediator. In other words, condition (1.1) means that the considered $2 \rightarrow 2$ process can be decomposed into a sequence of a decay and an inverse decay, as depicted in fig. 1, with all particles on-shell.

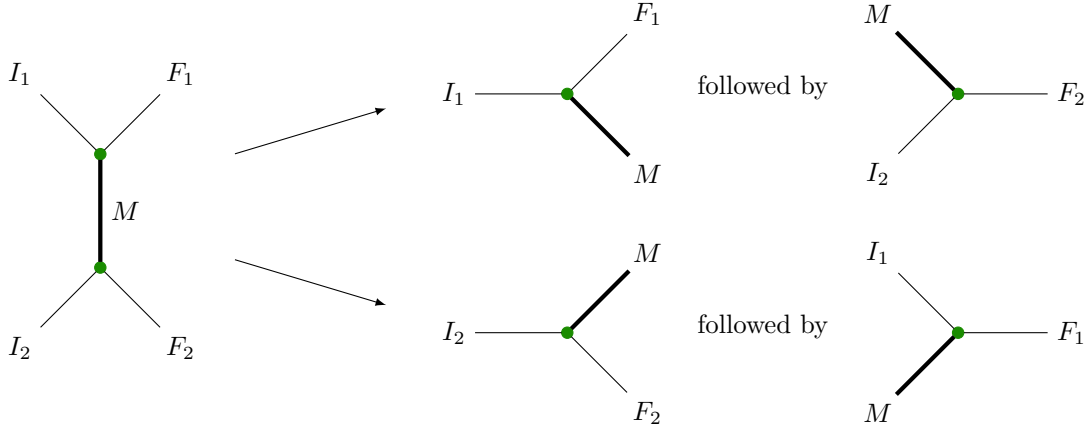


Figure 1. Possible decompositions of a $2 \rightarrow 2$ t -channel process with an on-shell mediator (M , distinguished with a thick line), corresponding to condition (1.1).

The paper [16] proves the above statement and presents a method to regularize the t -channel singularity. The method bases on applying the real-time (Keldysh-Schwinger) formalism to calculate a temperature-dependent one-loop mediator's self-energy which is a result of thermal interactions between the mediator and the surrounding medium. The

imaginary part of that self-energy prevents the mediator's propagator from being singular. That method is particularly useful if the singularity appears in cosmological considerations, e.g., those involving hypothetical dark matter particles.

1.3 This paper

The aforementioned results of [16] are calculated for the case of a scalar mediator and scalar loop states. In this work, the method presented there is generalized to the case of particles of spin 0, $1/2$, and 1. The method is illustrated with calculation of particles' self-energies within the Vector-Fermion Dark Matter model [17].

The paper is organized as follows. In section 2, a definition of an effective width is provided. The effective width is obtained from the imaginary part of the resummed propagator's denominator and expressed in terms of the mediator's self-energy. Section 3 contains calculation of the effective width within the Keldysh-Schwinger formalism and presents analytical results depending on particles' spins, expressed using a model-dependent factor X_0 . In section 4, the model-dependent factor X_0 is calculated within the Vector-Fermion Dark Matter model [17]. Section 5 contains summary and conclusions. The appendices present Green's functions used in the Keldysh-Schwinger formalism (appendix B) and contain some details of calculations from the previous sections (appendices C and E). Appendix D provides the general expression for the aforementioned factor X_0 , while in appendix F the result obtained in this paper is compared to the one from [14].

2 Dyson resummation. Effective width in terms of the particle's self-energy

The goal of this section is to calculate a resummed propagator (see fig. 2) containing an infinite sum of self-energy corrections. Then, the dependence between the effective width and the self-energy is concluded.

The self-energy Π^+ used in section 3 to perform the regularization is the *retarded one-loop* self-energy calculated within the Keldysh-Schwinger formalism, as explained in [16, 18]. In this section, however, the resummation is performed without any assumptions about the nature of Π^+ .

Let p , T denote the momentum of the particle and the temperature of the medium, respectively. For a scalar (spin-0) state, the resummed propagator is given by

$$\begin{aligned} i\Delta(p, T) &\equiv i\Delta^{(0)}(p) \sum_{n=0}^{\infty} \left[i\Pi^+(p, T) i\Delta^{(0)}(p) \right]^n \\ &= i\Delta^{(0)}(p) \left[1 - i\Pi^+(p, T) i\Delta^{(0)}(p) \right]^{-1}, \end{aligned} \quad (2.1)$$

while for a fermion (spin- $1/2$)

$$\begin{aligned} iG(p, T) &\equiv iG^{(0)}(p) \sum_{n=0}^{\infty} \left[i\Pi^+(p, T) iG^{(0)}(p) \right]^n \\ &= iG^{(0)}(p) \left[1 - i\Pi^+(p, T) iG^{(0)}(p) \right]^{-1}, \end{aligned} \quad (2.2)$$

and for a vector (spin-1)

$$\begin{aligned}
iD_{\mu\nu}(p, T) &\equiv iD_{\mu\alpha}^{(0)}(p) \left(\sum_{n=0}^{\infty} \left[i\Pi^+(p, T) iD^{(0)}(p) \right]^n \right)^{\alpha}_{\nu} \\
&= iD_{\mu\alpha}^{(0)}(p) \left(\left[1 - i\Pi^+(p, T) iD^{(0)}(p) \right]^{-1} \right)^{\alpha}_{\nu}.
\end{aligned} \tag{2.3}$$

$$\begin{aligned}
--\frac{i\Delta}{p}-- &= --\frac{i\Delta^{(0)}}{p}-- + --\frac{i\Delta^{(0)}}{p}-- \text{blob} --\frac{i\Delta^{(0)}}{p}-- + --\frac{i\Delta^{(0)}}{p}-- \text{blob} --\frac{i\Delta^{(0)}}{p}-- \text{blob} --\frac{i\Delta^{(0)}}{p}-- + \dots \\
\frac{iG}{p} &= \frac{iG^{(0)}}{p} + \frac{iG^{(0)}}{p} \text{blob} \frac{iG^{(0)}}{p} + \frac{iG^{(0)}}{p} \text{blob} \frac{iG^{(0)}}{p} \text{blob} \frac{iG^{(0)}}{p} + \dots \\
\sim\frac{iD}{p}\sim &= \sim\frac{iD^{(0)}}{p}\sim + \sim\frac{iD^{(0)}}{p}\sim \text{blob} \sim\frac{iD^{(0)}}{p}\sim + \sim\frac{iD^{(0)}}{p}\sim \text{blob} \sim\frac{iD^{(0)}}{p}\sim \text{blob} \sim\frac{iD^{(0)}}{p}\sim + \dots
\end{aligned}$$

Figure 2. Feynman diagrams corresponding to the resummed propagators of a scalar (top), a fermion (center), and a vector (bottom) mediator. The green blobs denote self-energy contributions.

Here, $\Delta^{(0)}, G^{(0)}, D^{(0)}$ denote the bare propagator of a given field (scalar, fermion, or vector, respectively) and Π^+ is the self-energy (which is calculated in section 3). Since particles propagating through a thermal¹ medium are considered here, the self-energy can depend on the particle's momentum, p , and the temperature of the medium, T .

Note that for a scalar or vector state, dimension of the self-energy is energy squared, while for a fermion state the dimension is the first power of energy.

The following sections 2.1 to 2.3 provide explicit expressions for the resummed propagator in each case. Mass of the particle is denoted by M .

2.1 Scalar state

In the scalar case, both $\Delta^{(0)}$ and Π^+ are scalar quantities:

$$\Delta^{(0)}(p) = \frac{1}{p^2 - M^2}, \tag{2.4}$$

so from eq. (2.1) one obtains

$$\Delta(p, T) = \frac{1}{p^2 - M^2 + \Pi^+(p, T)}. \tag{2.5}$$

¹ In fact, the convenient assumption that the medium is in thermal equilibrium is not necessary. The self-energies and, consequently, the effective widths can be calculated for non-thermally distributed energies of the medium's particles as well, assuming different form of distribution functions $n_{F,B}$ in appendix B.

2.1.1 Thermal tree-level propagator vs. the zero-temperature formula

In general, the tree-level scalar propagator contains a statistical part proportional to $\delta(p^2 - m^2)$ (see, e.g., appendix A.4 of [19]):

$$\begin{aligned}\Delta_{\text{th}}^{(0)}(p) &\equiv \frac{1}{p^2 - M^2} - 2\pi i n(E_p) \delta(p^2 - M^2) \\ &= \Delta^{(0)}(p) [1 - 2\pi i n(E_p) (p^2 - M^2) \delta(p^2 - M^2)] ,\end{aligned}\tag{2.6}$$

where $n(E_p)$ is the distribution function:

$$n(E_p) \equiv [e^{\beta E_p} - 1]^{-1} , \quad E_p \equiv \sqrt{\mathbf{p}^2 + m^2} ,\tag{2.7}$$

and $\Delta^{(0)}(p)$ is the propagator given by eq. (2.4). Then, the resummed propagator calculated using the $\Delta_{\text{th}}^{(0)}$ bare propagator becomes:

$$\begin{aligned}\Delta &= \Delta_{\text{th}}^{(0)} \left[1 + \Pi^+ \Delta_{\text{th}}^{(0)} \right]^{-1} \\ &= \Delta^{(0)} [1 - 2\pi i n(E_p) (p^2 - M^2) \delta(p^2 - M^2)] \\ &\quad \times \left[1 + \Pi^+ \Delta^{(0)} - 2\pi i \Pi^+ n(E_p) \delta(p^2 - M^2) \right]^{-1} \\ &= \frac{1 - 2\pi i n(E_p) (p^2 - M^2) \delta(p^2 - M^2)}{p^2 - M^2 + \Pi^+ - 2\pi i \Pi^+ n(E_p) (p^2 - M^2) \delta(p^2 - M^2)} .\end{aligned}\tag{2.8}$$

As long as Π^+ is regular (i.e., finite, non-zero and smooth enough) at $p^2 = M^2$, all the above operations are legal and the $(p^2 - M^2) \delta(p^2 - M^2)$ component can be dropped² both in the numerator and the denominator of the above expression, which provides the same result as obtained for the zero-temperature bare propagator (2.4). Therefore, the statistical component could have been neglected from the very beginning. The same logic applies to the fermion and vector cases.

2.2 Fermion state

In the fermion case, $G^{(0)}$ and Π^+ possess spinor structure. They can³ be expressed using the gamma matrices as

$$G^{(0)}(p) = \frac{1}{\not{p} - M} ,\tag{2.9}$$

$$\Pi^+(p, T) = [A_v(p, T) + A_a(p, T)\gamma_5] \not{p} + [B_v(p, T) + B_a(p, T)\gamma_5] M ,$$

where $A_{v,a}$ and $B_{v,a}$ are dimensionless scalar quantities and $\not{p} \equiv p^\mu \gamma_\mu$. According to eq. (2.2), the resummed propagator is given by

$$\begin{aligned}iG &= iG^{(0)} \left[1 - i\Pi^+ iG^{(0)} \right]^{-1} \\ &= i \frac{1}{\not{p} - M} \left[\frac{(1 + A_v + A_a \gamma_5) \not{p} + (-1 + B_v + B_a \gamma_5) M}{\not{p} - M} \right]^{-1} \\ &= i \frac{(1 + A_v + A_a \gamma_5) \not{p} + (1 - B_v + B_a \gamma_5) M}{[(1 + A_v)^2 - A_a^2] p^2 - [(1 - B_v)^2 - B_a^2] M^2} .\end{aligned}\tag{2.10}$$

²This is because $f(x) = x \delta(x)$ is equivalent to zero in the distributional sense. Hence, as long as it is multiplied by regular functions only, such a term must vanish in comparison to any non-zero term.

³For a brief discussion, see section A of chapter III in [20].

Hence,

$$G(p, T) = \frac{[1 + A_v(p, T) + A_a(p, T) \gamma_5] \not{p} + [1 - B_v(p, T) + B_a(p, T) \gamma_5] M}{\left([1 + A_v(p, T)]^2 - A_a(p, T)^2\right) p^2 - \left([1 - B_v(p, T)]^2 - B_a(p, T)^2\right) M^2} . \quad (2.11)$$

To simplify this formula, let us assume that:

- the self-energy is small comparing to the mass: $|A_{v,a}| \ll 1, |B_{v,a}| \ll 1$,
- the axial coefficients of the self-energy are at most of the order of the vector coefficients: $|A_a|, |B_a| \lesssim |A_v|, |B_v|$,
- the singular propagator is almost on-shell:⁴ $|p^2 - M^2| \ll M^2$.

Under these assumptions one obtains⁵

$$G(p, T) \simeq \frac{\not{p} + M}{p^2 - M^2 + 2[A_v(p, T) + B_v(p, T)] M^2} . \quad (2.12)$$

Note that A_v and B_v can be calculated from the self-energy using the trace operator:

$$A_v(p, T) = \frac{1}{4p^2} \text{tr}[\not{p} \Pi^+(p, T)] , \quad B_v(p, T) = \frac{1}{4M} \text{tr}[\Pi^+(p, T)] , \quad (2.13)$$

so

$$\boxed{G(p, T) \simeq \frac{\not{p} + M}{p^2 - M^2 + 2 \text{tr} \left[\frac{\not{p} + M}{4} \Pi^+(p, T) \right]}} . \quad (2.14)$$

2.3 Vector state

In the vector case, $D^{(0)}$ and Π^+ have Lorentz structure and can be conveniently expressed as

$$\begin{aligned} D_{\mu\nu}^{(0)}(p) &= - \left(\frac{T_{\mu\alpha}}{p^2 - M^2} - \frac{L_{\mu\alpha}}{M^2} \right) , \\ \Pi_{\mu\nu}^+(p) &= \Pi_T(p, T) T_{\mu\nu} + \Pi_L(p, T) L_{\mu\nu} , \end{aligned} \quad (2.15)$$

where Π_T and Π_L , denoting the transverse and the longitudinal component of the self-energy, respectively, are scalar quantities of dimension of energy squared. The transverse projector $T_{\mu\nu}$ and the longitudinal projector $L_{\mu\nu}$ are defined as

$$T_{\mu\nu} \equiv g_{\mu\nu} - \frac{p_\mu p_\nu}{p^2} , \quad L_{\mu\nu} \equiv \frac{p_\mu p_\nu}{p^2} . \quad (2.16)$$

⁴This is assumed basing on the fact that the vicinity of the singular point dominates the momentum-space integral.

⁵This result agrees with eq. (11) of [21]. Note that their A, B are here $-B_v M, -A_v$, respectively.

Then, according to eq. (2.3),

$$\begin{aligned}
iD_{\mu\nu} &= iD_{\mu\alpha}^{(0)} \left(\left[1 - i\Pi^+(p, T) iD^{(0)}(p) \right]^{-1} \right)_{\nu}^{\alpha} \\
&= -i \left(\frac{T_{\mu\alpha}}{p^2 - M^2} - \frac{L_{\mu\alpha}}{M^2} \right) \left(\left[\frac{p^2 - M^2 - \Pi_T}{p^2 - M^2} T + \frac{M^2 + \Pi_L}{M^2} L \right]^{-1} \right)_{\nu}^{\alpha} \\
&= -i \left(\frac{T_{\mu\alpha}}{p^2 - M^2} - \frac{L_{\mu\alpha}}{M^2} \right) \left[\frac{p^2 - M^2}{p^2 - M^2 - \Pi_T} T_{\nu}^{\alpha} + \frac{M^2}{M^2 + \Pi_L} L_{\nu}^{\alpha} \right] \\
&= -i \frac{T_{\mu\nu}}{p^2 - M^2 - \Pi_T} + i \frac{L_{\mu\nu}}{M^2 + \Pi_L} \\
&= i \frac{-g_{\mu\nu} + \frac{p_{\mu}p_{\nu}}{M^2 + \Pi_L} \frac{p^2 - \Pi_T + \Pi_L}{p^2}}{p^2 - M^2 - \Pi_T} ,
\end{aligned} \tag{2.17}$$

so⁶

$$D_{\mu\nu}(p, T) = \frac{-g_{\mu\nu} + \frac{p_{\mu}p_{\nu}}{M^2 + \Pi_L(p, T)} \frac{p^2 - \Pi_T(p, T) + \Pi_L(p, T)}{p^2}}{p^2 - M^2 - \Pi_T(p, T)} . \tag{2.18}$$

Assuming that the self-energy is small (i.e., $|\Pi_L|, |\Pi_T| \ll M^2$) and the propagating state is almost on-shell (so that $|p^2 - M^2| \ll M^2$), one obtains

$$D_{\mu\nu}(p, T) \simeq \frac{-g_{\mu\nu} + \frac{p_{\mu}p_{\nu}}{M^2}}{p^2 - M^2 - \Pi_T(p, T)} . \tag{2.19}$$

Quantity Π_T can be expressed as

$$\Pi_T(p, T) = \frac{1}{3} \left(g^{\mu\nu} - \frac{p^{\mu}p^{\nu}}{p^2} \right) \Pi_{\mu\nu}^+(p, T) , \tag{2.20}$$

so

$$D_{\mu\nu}(p, T) \simeq \frac{-g_{\mu\nu} + \frac{p_{\mu}p_{\nu}}{M^2}}{p^2 - M^2 + \frac{1}{3} \left(-g^{\alpha\beta} + \frac{p^{\alpha}p^{\beta}}{p^2} \right) \Pi_{\alpha\beta}^+(p, T)} . \tag{2.21}$$

2.4 Effective width

The imaginary part of the expression that is present in the resummed propagator but absent in the free propagator can be denoted as $\Sigma(p, T)$:

$$\Sigma(p, T) \equiv \begin{cases} \Im \Pi^+(p, T) & \text{scalar case} \\ \Im \left(\text{tr} \left[\frac{\not{p} + M}{2} \Pi^+(p, T) \right] \right) & \text{fermion case} \\ \Im \left[\frac{1}{3} \left(-g^{\mu\nu} + \frac{p^{\mu}p^{\nu}}{p^2} \right) \Pi_{\mu\nu}^+(p, T) \right] & \text{vector case} \end{cases} . \tag{2.22}$$

In each case, in an analogy to the Breit-Wigner propagator, a (p, T) -dependent effective decay width $\Gamma_{\text{eff}}(p, T)$ can be introduced in the following way:

$$\Gamma_{\text{eff}}(p, T) \equiv \frac{|\Sigma(p, T)|}{M} . \tag{2.23}$$

⁶This result agrees with eq. (20) of [22], up to the sign of Π_T in their equation. Note that their $\Pi_T(q^2)$ is equal to $\Pi_T(q^2)$ used here, while their $\Pi_L(q^2)$ is here $[\Pi_L(q^2) - \Pi_T(q^2)]/q^2$.

If this quantity is non-zero, it regularizes the singular on-shell propagator in the very same manner as the Breit-Wigner propagator is regularized by the standard decay width.

Note that the real part of the expression changes the value of mass, e.g., the bare mass M^2 becomes $M^2 - \Re\Pi^+(p, T)$ in the scalar case. Hence, strictly speaking, from now on, M^2 denotes the dressed mass. Nevertheless, it is assumed that the shift is small in comparison to the bare mass M^2 , so that the kinematics of the process involving the considered particle is not affected qualitatively (in particular, condition (1.1) still applies if did before).

3 Calculation of the regulator $\Sigma(p, T)$

In the statistical field theory, the Boltzmann equation appears as a semi-classical approximation of the so-called Kadanoff-Baym equations [23] (for a derivation of the Boltzmann equation see also section 10 of [24]), which are equations of motion of thermal Green's functions. The amplitude of the discussed t -channel process shown in fig. 1 enters those equations as a part of the contribution corresponding to the self-energy of one of the external particles. Figure 3 shows the relation between the self-energy of particle I_1 and the amplitude of the process. The propagator of the mediator, singular in the usual treatment, has to be replaced by the statistical counterpart. In this paper, this is achieved by including in the resummed propagator the one-loop retarded self-energy calculated within the Keldysh-Schwinger formalism.

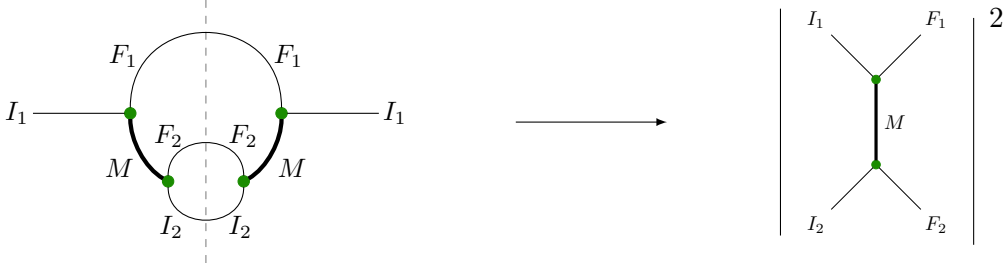


Figure 3. Relation between the self-energy of particle I_1 and the amplitude of the considered t -channel process $I_1 I_2 \rightarrow F_1 F_2$. The dashed line represents the corresponding cut of the self-energy diagram. For clarity, the line representing the t -channel mediator is thickened.

This section provides a result for the effective width $\Gamma_{\text{eff}} \equiv |\Sigma|/M$, defined by eq. (2.23), obtained for Π^+ denoting the thermal self-energy.

Let us denote the mediator's mass by M , its four-momentum measured in the rest frame of the medium by $p = (p_0, \mathbf{p})$, and the states present in the loop by 1 and 2 (with masses m_1 and m_2 , respectively), see fig. 4.

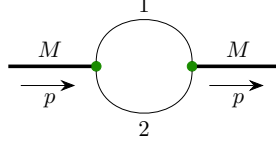


Figure 4. Diagram of the mediator's one-loop self-energy.

For convenience, one can define

$$\beta \equiv \frac{1}{T}, \quad E_p \equiv \sqrt{\mathbf{p}^2 + M^2}, \quad E_{1,2} \equiv \sqrt{\mathbf{k}^2 + m_{1,2}^2}. \quad (3.1)$$

Because the process is expected to be t -channel singular, it is assumed that the mediator is (almost) on-shell, so

$$p_0 = E_p, \quad p^2 = M^2, \quad (3.2)$$

and stable in vacuum:

$$M < m_1 + m_2. \quad (3.3)$$

If all three states are scalars and the vertex factor is μ , the mediator's retarded one-loop self-energy $\Pi^+(x)$ calculated within the Keldysh-Schwinger formalism can be found (see [16]) as

$$\Pi^+(p, T) = \frac{i}{2} \int \frac{d^4 k}{(2\pi)^4} \left[\mu \Delta_1^+(k+p) \mu \Delta_2^{\text{sym}}(k, T) + \mu \Delta_1^{\text{sym}}(k, T) \mu \Delta_2^-(k-p) \right]. \quad (3.4)$$

If the particles (the mediator and the loop states) have non-zero spins, the self-energy can be found analogously, using $G(D_{\mu\nu})$ as a fermion (vector) propagator and replacing μ by an appropriate vertex contribution.

The retarded, advanced, and symmetric Green's functions for scalar, fermion, and vector particles: $\Delta^\pm(p)$, $G^\pm(p)$, $D_{\mu\nu}^\pm(p)$, and $\Delta^{\text{sym}}(p, T)$, $G^{\text{sym}}(p, T)$, $D_{\mu\nu}^{\text{sym}}(p, T)$ are provided in appendix B. Substituting them into eq. (3.4) will allow us to obtain $\Pi^+(p, T)$ needed to calculate Σ defined by eq. (2.22).

According to eq. (2.22), in the case of a scalar mediator the result of eq. (3.4) is what is needed to calculate Σ . In the case of a fermion mediator one has to multiply the result by $\frac{\not{p} + M}{2}$ and calculate the trace, while in the case of a vector mediator the result has to be multiplied by $\frac{1}{3} \left(-g^{\mu\nu} + \frac{p^\mu p^\nu}{p^2} \right)$. Then, in each case, the imaginary part should be found. Regardless of the case, the effect of these manipulations can be expressed as

$$\begin{aligned} \Sigma(p, T) = \Im \left[\frac{1}{2} \int \frac{d^4 k}{(2\pi)^4} \left\{ \frac{X_{(p^2, k^2, (k+p)^2)}}{(k+p)^2 - m_1^2 + i \operatorname{sgn}(k_0 + p_0) 0^+} \right. \right. \\ \times \frac{\pi}{E_2} \left(\delta(E_2 - k_0) + \delta(E_2 + k_0) \right) f_2(\beta E_2) \\ + \frac{X_{(p^2, (k-p)^2, p^2)}}{(k-p)^2 - m_2^2 - i \operatorname{sgn}(k_0 - p_0) 0^+} \\ \left. \times \frac{\pi}{E_1} \left(\delta(E_1 - k_0) + \delta(E_1 + k_0) \right) f_1(\beta E_1) \right\} \right], \end{aligned} \quad (3.5)$$

where function f_i is defined as

$$f_i(x) \equiv \begin{cases} \frac{e^x - 1}{e^x + 1} & \text{if particle } i \text{ is a fermion} \\ \frac{e^x + 1}{e^x - 1} & \text{if particle } i \text{ is a boson} \end{cases}, \quad (3.6)$$

while the Lorentz invariant X , being a product of appropriate coupling constants and numerators of the propagators after applying the procedure mentioned above eq. (3.5), has to be calculated within a given model.

The integration over d^4k makes the result insensitive to the direction of \mathbf{p} , so the imaginary part of the self-energy becomes energy-dependent:

$$\Sigma(p, T) = \Sigma(E_p, T). \quad (3.7)$$

Integrating over k_0 one finds

$$\begin{aligned} \Sigma(E_p, T) = \Im \left[\frac{1}{4} \int \frac{d^3k}{(2\pi)^3} \left\{ \frac{X_{(p^2, k^2, (k+p)^2)}}{E_2} f_2(\beta E_2) \right. \right. \\ \times \left[\frac{1}{M^2 + m_2^2 - m_1^2 + 2pk + i \operatorname{sgn}(E_2 + E_p) 0^+} \right. \\ \left. \left. + \frac{1}{M^2 + m_2^2 - m_1^2 + 2pk + i \operatorname{sgn}(-E_2 + E_p) 0^+} \right] \right. \\ \left. + \frac{X_{(p^2, (k-p)^2, k^2)}}{E_1} f_1(\beta E_1) \right. \\ \times \left[\frac{1}{M^2 - m_2^2 + m_1^2 - 2pk - i \operatorname{sgn}(E_1 - E_p) 0^+} \right. \\ \left. \left. + \frac{1}{M^2 - m_2^2 + m_1^2 - 2pk - i \operatorname{sgn}(-E_1 - E_p) 0^+} \right] \right\} \Bigg]. \quad (3.8) \end{aligned}$$

Due to the Sochocki relation:

$$\lim_{\varepsilon \rightarrow 0^+} \frac{1}{x \pm i\varepsilon} = \mathcal{P} \frac{1}{x} \mp i\pi \delta(x), \quad (3.9)$$

the result equals to

$$\begin{aligned} \Sigma(E_p, T) = \frac{\pi}{4} \int \frac{d^3k}{(2\pi)^3} \left\{ -X_0 f_2(\beta E_2) \left[\frac{\operatorname{sgn}(E_2 + E_p)}{E_2} + \frac{\operatorname{sgn}(-E_2 + E_p)}{E_2} \right] \right. \\ \times \delta(M^2 + m_2^2 - m_1^2 + 2pk) \\ X_0 f_1(\beta E_1) \left[\frac{\operatorname{sgn}(E_1 - E_p)}{E_1} + \frac{\operatorname{sgn}(-E_1 - E_p)}{E_1} \right] \\ \left. \times \delta(M^2 - m_2^2 + m_1^2 - 2pk) \right\}, \quad (3.10) \end{aligned}$$

where X_0 is the on-shell value of X :

$$X_0 \equiv X_{(M^2, m_2^2, m_1^2)}. \quad (3.11)$$

For further calculations, the spherical coordinates with the z axis set along the vector \mathbf{p} are used: instead of d^3k , integration over $\mathbf{k}^2 d|\mathbf{k}| d\cos\theta d\varphi$ is performed, with the angles θ and φ defined via the following relations:

$$\begin{aligned} p^\mu &= (E_p = \sqrt{\mathbf{p}^2 + M^2}, 0, 0, |\mathbf{p}|), \\ k^\mu &= (k_0, |\mathbf{k}| \sin\theta \cos\varphi, |\mathbf{k}| \sin\theta \sin\varphi, |\mathbf{k}| \cos\theta). \end{aligned} \quad (3.12)$$

In this coordinate system, the Lorentz invariants are given by

$$p^\mu p_\mu = M^2, \quad k^\mu k_\mu = k_0^2 - \mathbf{k}^2, \quad p^\mu k_\mu = E_p k_0 - |\mathbf{k}||\mathbf{p}| \cos\theta. \quad (3.13)$$

It is now assumed that $\mathbf{p} \neq 0$.⁷ The integral over the azimuthal angle φ is trivial and the remaining integrals are

$$\begin{aligned} \Sigma(E_p, T) &= \frac{X_0}{32\pi} \int_0^\infty \mathbf{k}^2 d|\mathbf{k}| \int_{-1}^1 d\cos\theta \\ &\times \left\{ -f_2(\beta E_2) \left[\frac{\text{sgn}(E_2 + E_p)}{E_2} \frac{\delta(\cos\theta - \cos\alpha_2)}{|\mathbf{k}||\mathbf{p}|} \right. \right. \\ &\quad \left. \left. + \frac{\text{sgn}(-E_2 + E_p)}{E_2} \frac{\delta(\cos\theta - \cos\beta_2)}{|\mathbf{k}||\mathbf{p}|} \right] \right. \\ &\quad \left. + f_1(\beta E_1) \left[\frac{\text{sgn}(E_1 - E_p)}{E_1} \frac{\delta(\cos\theta - \cos\alpha_1)}{|\mathbf{k}||\mathbf{p}|} \right. \right. \\ &\quad \left. \left. + \frac{\text{sgn}(-E_1 - E_p)}{E_1} \frac{\delta(\cos\theta - \cos\beta_1)}{|\mathbf{k}||\mathbf{p}|} \right] \right\} \\ &= \frac{X_0}{32\pi|\mathbf{p}|} \left\{ - \int_0^\infty dE_2 \int_{-1}^1 d\cos\theta f_2(\beta E_2) \right. \\ &\quad \times \left[\text{sgn}(E_2 + E_p) \delta(\cos\theta - \cos\alpha_2) \right. \\ &\quad \left. \left. + \text{sgn}(-E_2 + E_p) \delta(\cos\theta - \cos\beta_2) \right] \right. \\ &\quad \left. + \int_0^\infty dE_1 \int_{-1}^1 d\cos\theta f_1(\beta E_1) \right. \\ &\quad \times \left[\text{sgn}(E_1 - E_p) \delta(\cos\theta - \cos\alpha_1) \right. \\ &\quad \left. \left. + \text{sgn}(-E_1 - E_p) \delta(\cos\theta - \cos\beta_1) \right] \right\} \end{aligned} \quad (3.14)$$

where

$$\begin{aligned} \cos\alpha_1 &\equiv \frac{-(m_1^2 - m_2^2 + M^2) + 2E_1 E_p}{2|\mathbf{k}||\mathbf{p}|}, \quad \cos\beta_1 \equiv \frac{-(m_1^2 - m_2^2 + M^2) - 2E_1 E_p}{2|\mathbf{k}||\mathbf{p}|}, \\ \cos\alpha_2 &\equiv \frac{-(m_1^2 - m_2^2 - M^2) + 2E_2 E_p}{2|\mathbf{k}||\mathbf{p}|}, \quad \cos\beta_2 \equiv \frac{-(m_1^2 - m_2^2 - M^2) - 2E_2 E_p}{2|\mathbf{k}||\mathbf{p}|}. \end{aligned} \quad (3.15)$$

Since the integrand depends on $\cos\theta$ via $\delta(\cos\theta - \cos\alpha_i)$ or $\delta(\cos\theta - \cos\beta_i)$ functions ($i = 1, 2$) only, the integration over $d\cos\theta$ effectively limits the range of $E_{1,2}$ to the values

⁷The other case is easy to solve and appears to be a limit of this one; the result is provided in eq. (3.25).

leading to $|\cos \alpha_i| < 1$ or $|\cos \beta_i| < 1$. In appendix C, it is proved that this range is non-empty only if

$$m_1 > m_2 + M \quad (3.16)$$

or

$$m_2 > m_1 + M . \quad (3.17)$$

Because the existence of a particle that is allowed to decay into the mediator and another particle is necessary for the singularity to occur (see condition (1.1)), it is possible to find two states of masses m_1 and m_2 that satisfy one of the above conditions. Hence, if the t -channel singularity occurs, it can always be regularized using the method presented in this paper. Without loss of generality, one can assume that ineq. (3.16) holds, so the particle of mass m_1 can decay as $m_1 \rightarrow m_2 + M$. Also the inverse process $m_2 + M \rightarrow m_1$ is kinematically allowed. Note that in section 3.1 it is shown that in the limit of $m_1 = m_2 + M$ the thermal self-energy vanishes.

As shown in appendix C, given that ineq. (3.16) holds, the terms containing deltas with $\cos \beta_{1,2}$ vanish and the remaining part can be expressed as

$$\begin{aligned} \Sigma(E_p, T) = \frac{X_0}{32\pi} \frac{1}{|\mathbf{p}|} & \left[- \int_{b-a-E_p}^{b+a-E_p} dE_2 f_2(\beta E_2) \text{sgn}(E_2 + E_p) \right. \\ & \left. + \int_{b-a}^{b+a} dE_1 f_1(\beta E_1) \text{sgn}(E_1 - E_p) \right] , \end{aligned} \quad (3.18)$$

with a and b defined as

$$\begin{aligned} a &\equiv \frac{\lambda(m_1^2, m_2^2, M^2)^{1/2}}{2M^2} |\mathbf{p}| , & b &\equiv \frac{m_1^2 - m_2^2 + M^2}{2M^2} E_p , \\ \lambda(m_1^2, m_2^2, M^2) &\equiv [m_1^2 - (m_2 - M)^2] [m_1^2 - (m_2 + M)^2] . \end{aligned} \quad (3.19)$$

The sgn function in the first integral of eq. (3.18) gives, obviously, +1, and since

$$b - a - E_p > 0 , \quad (3.20)$$

(see eq. (C.12)), the second sgn function gives +1 as well. Therefore, the imaginary part of the self-energy becomes

$$\begin{aligned} \Sigma(E_p, T) &= \frac{X_0}{32\pi} \frac{1}{|\mathbf{p}|} \left[- \int_{b-a-E_p}^{b+a-E_p} dE_2 f_2(\beta E_2) + \int_{b-a}^{b+a} dE_1 f_1(\beta E_1) \right] \\ &= \frac{X_0}{32\pi} \frac{1}{\beta |\mathbf{p}|} \left[\int_{\beta(b-a)}^{\beta(b+a)} f_1(x) dx - \int_{\beta(b-a-E_p)}^{\beta(b+a-E_p)} f_2(x) dx \right] , \end{aligned} \quad (3.21)$$

where

$$f_i(x) \equiv \begin{cases} \frac{e^x + 1}{e^x - 1} & \text{particle } i \text{ is a boson} \\ \frac{e^x - 1}{e^x + 1} & \text{particle } i \text{ is a fermion} \end{cases} , \quad i = 1, 2 . \quad (3.22)$$

After integration, the final result, depending on the spins of the particles in the loop, is given as

$$\begin{aligned}
\Gamma_{\text{eff}}(E_p, T) &\equiv \frac{1}{M} |\Sigma(E_p, T)|, \\
\Sigma(E_p, T) &= \frac{1}{16\pi} \frac{X_0}{\beta |\mathbf{p}|} \left[\ln \frac{e^{\beta(b+a)} + \eta_1}{e^{\beta(b-a)} + \eta_1} - \ln \frac{e^{\beta(b+a)} e^{-\beta E_p} + \eta_2}{e^{\beta(b-a)} e^{-\beta E_p} + \eta_2} \right] \\
&= \frac{1}{16\pi} \frac{X_0}{\beta |\mathbf{p}|} \ln \left[1 + \frac{e^{-\beta(b-a)} e^{\beta E_p} (1 - e^{-2\beta a}) (\eta_2 - \eta_1 e^{-\beta E_p})}{(1 + \eta_1 e^{-\beta(b-a)}) (1 + \eta_2 e^{-\beta(b+a)} e^{\beta E_p})} \right],
\end{aligned} \tag{3.23}$$

where

$$\begin{aligned}
\eta_i &\equiv \begin{cases} -1 & \text{particle } i \text{ is a boson} \\ +1 & \text{particle } i \text{ is a fermion} \end{cases}, \\
\beta &\equiv \frac{1}{T}, \quad |\mathbf{p}| \equiv \sqrt{E_p^2 - M^2}, \\
a &\equiv \frac{|\mathbf{p}| \sqrt{\lambda(m_1^2, m_2^2, M^2)}}{2M^2}, \quad b \equiv \frac{m_1^2 - m_2^2 + M^2}{2M^2} E_p, \\
\lambda(m_1^2, m_2^2, M^2) &\equiv [m_1^2 - (m_2 - M)^2] [m_1^2 - (m_2 + M)^2],
\end{aligned} \tag{3.24}$$

M denotes the mediator's mass and X_0 is defined in eq. (3.11). Values of X_0 are provided, for the general case, in appendix D, and for the Vector-Fermion Dark Matter model [17] in appendix E and section 4.

3.1 Result discussion

The above result is consistent with that derived in [14] up to a spin-dependent factor of $1/2$ for a fermion mediator and $1/3$ for a vector mediator, see appendix F.

As it is clear from the last line of eq. (3.23), the logarithmic part is positive if the particle „2” is a fermion and negative otherwise, given that $m_1 > m_2 + M$ (ineq. (3.16)) and $b > a + E_p$ (ineq. (3.20)). This corresponds to the sign of the factor X_0 calculated in appendix D. Consequently, in any model consisting of scalars, fermions and vectors, the regulator Σ is always positive and regularizes the singularity (therefore, the absolute value in eq. (3.23) can be omitted).

If $m_1 = m_2 + M$, quantity a vanishes and so does the effective width (as expected, since non-zero effective width is a consequence of a decay of particle „1” into „2” and the mediator, see ineq. (3.16)).

Note that values of eq. (3.23) for $\eta_1 = -\eta_2 = 1$ and for $\eta_1 = -\eta_2 = -1$ are not identical, even though both assume a boson and a fermion in the loop. The difference is that in the first case the particle allowed to decay is the fermion, while in the second case the decaying particle is the boson, which leads to a different statistical factor that has to be taken into account in each case.

In the limit of $\beta \rightarrow \infty$ (zero-temperature limit), the result tends to 0 (the argument of the logarithmic function in the last line becomes 1). This behaviour is expected, as the

thermal width is a result of interactions between the mediator and a medium of non-zero temperature. Taking $\beta \rightarrow \infty$ reflects lack of the medium.

The same happens in the limit of $|\mathbf{p}| \rightarrow \infty$. Physically, the process is regularized by interactions between the mediator and the thermal bath. The calculated self-energy represent destruction of the mediator due to interaction with particle „2” (from the thermal bath), with production of particle „1”, and a subsequent decay of particle „1” into particle „2” and mediator of exactly the same energy as the destroyed one. Ineq. (C.11) provides the minimal value of energy E_2 necessary for an on-shell production of particle „1” in a $M, 2 \rightarrow 1$ process (with the mediator having energy E_p), which is $b - a - E_p$. As $|\mathbf{p}|$ goes to infinity, this minimal energy tends to infinity as well, so only a small amount of particles in the thermal bath is energetic enough. This leads to statistical suppression of the regulator.

In the limit of $\mathbf{p} \rightarrow 0$ (zero-momentum limit), factor a is equal to 0, so the logarithmic function present in the result also tends to 0. However, p appears not only in a but also divides the results, so the overall limit can be non-trivial. In fact, it is equal to:

$$\Gamma_{\text{eff}}(\mathbf{p} = 0, T) = \frac{X_0}{16\pi M} \frac{\lambda(m_1^2, m_2^2, M^2)^{1/2}}{M^2} \frac{e^{-\beta(b_0 - M)} (\eta_2 - \eta_1 e^{-\beta M})}{(1 + \eta_1 e^{-\beta b_0}) (1 + \eta_2 e^{-\beta(b_0 - M)})}, \quad (3.25)$$

with $b_0 \equiv (m_1^2 - m_2^2 + M^2)/(2M) > M$.

If the temperature is small enough to ensure $\beta(b - a - E_p) \gtrsim 3$ (so that $e^{\beta(b - a - E_p)} \gg 1$), eq. (3.23) can be expanded around $e^{-\beta(b - a - E_p)} = 0$, giving

$$\Gamma_{\text{eff}}(E_p, T) \simeq \frac{1}{16\pi M} \frac{X_0}{\beta|\mathbf{p}|} e^{-\beta(b - a - E_p)} \left(1 - e^{-2\beta a}\right) \left(\eta_2 - \eta_1 e^{-\beta E_p}\right). \quad (3.26)$$

This form is especially useful for numerical calculations.

4 Values of the factor X_0 calculated within the VFDM model

In this section, the presented regularization method is illustrated by the results obtained for the case of the Vector-Fermion Dark Matter (VFDM) model [17], which extends the SM gauge group by an additional $U(1)_x$ with vector X serving as its gauge boson. In order to provide mass to X , the Higgs mechanism with a complex singlet S is employed. Scalar S mixes with the SM Higgs doublet H providing a Higgs portal that communicates SM to the dark sector. Diagonalizing the mass-squared matrix of the real-part fluctuations of S and H one obtains two mass eigenstates: h_1 identified with the known Higgs particle of mass 125 GeV, and h_2 whose mass can have, in principle, any value. The model also introduces two Majorana fermions denoted as ψ_+ and ψ_- , coupled to $h_{1,2}$ via Yukawa interaction with the coupling constant $y_x \equiv g_x(m_{\psi_+} - m_{\psi_-})/(2m_X)$, where g_x is the coupling constant of $U(1)_x$.

Particles X , ψ_+ and ψ_- , neutral under the action of the SM gauge group and charged under $U(1)_x$, can serve as dark matter candidates, interacting with the SM through a $h_{1,2}$ -mediated Higgs portal. Due to the presence of the $X\psi_+\psi_-$ interaction vertex, either two or three of those particles are stable, depending on whether the values of the masses allow one of them to decay into the two others.

The model parameters are masses of the potentially dark particles: m_X , m_{ψ_+} , m_{ψ_-} (by definition, m_{ψ_-} is always smaller than m_{ψ_+}), mass of the second Higgs state m_{h_2} , the $U(1)_x$ interaction constant g_x , and the sine of the scalar-sector mixing angle $\sin \alpha$.

Values of X_0 calculated within the VFDM model are presented in the following tables 1 to 3. A given loop contributes to the self-energy if the first of loop particles is allowed to decay into the second one and the mediator. For details of calculation of the results shown in the tables, see appendices D and E.

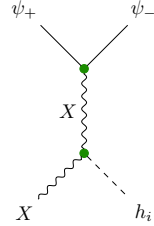
| mediator: X | | | singular process |
|----------------|--|---------------------------------|---|
| loop states | X_0 | condition |  |
| $\psi_+\psi_-$ | $\frac{1}{3} \mathcal{M} _{\psi_+\rightarrow X\psi_-}^2$ | $m_{\psi_+} > m_X + m_{\psi_-}$ | |
| $h_i X$ | $-\frac{1}{3} \mathcal{M} _{h_i\rightarrow XX}^2$ | $m_{h_i} > 2m_X$ | |

Table 1. Values of the factor X_0 calculated within the VFDM model for X being the mediator. Conditions for the loops to contribute to the effective width are also provided.

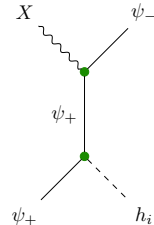
| mediator: ψ_+ | | | singular process |
|--------------------|---|---------------------------------|---|
| loop states | X_0 | condition |  |
| $X\psi_-$ | $\frac{1}{2} \mathcal{M} _{X\rightarrow\psi_+\psi_-}^2$ | $m_X > m_{\psi_+} + m_{\psi_-}$ | |
| $h_i\psi_+$ | $\frac{1}{2} \mathcal{M} _{h_i\rightarrow\psi_+\psi_+}^2$ | $m_{h_i} > 2m_{\psi_+}$ | |

Table 2. Values of the factor X_0 calculated within the VFDM model for ψ_+ being the mediator. Conditions for the loops to contribute to the effective width are also provided.

| mediator: ψ_- | | | singular process |
|--------------------|---|---------------------------------|------------------|
| loop states | X_0 | condition | |
| $X\psi_+$ | $\frac{1}{2} \mathcal{M} _{X \rightarrow \psi_+\psi_-}^2$ | $m_X > m_{\psi_+} + m_{\psi_-}$ | |
| ψ_+X | $-\frac{1}{2} \mathcal{M} _{\psi_+ \rightarrow X\psi_-}^2$ | $m_{\psi_+} > m_X + m_{\psi_-}$ | |
| $h_i\psi_-$ | $\frac{1}{2} \mathcal{M} _{h_i \rightarrow \psi_-\psi_-}^2$ | $m_{h_i} > 2m_{\psi_-}$ | |

Table 3. Values of the factor X_0 calculated within the VFDM model for ψ_- being the mediator. Conditions for the loops to contribute to the effective width are also provided.

For an illustration, the plots provided in fig. 5 show the values of Γ_{eff} calculated for particle X being the mediator. Figure 6 shows the cross section and the thermally averaged cross section calculated for the singular process $\psi_+X \rightarrow \psi_-h_2$ mediated by a t -channel X , regularized by the effective width shown in fig. 5.

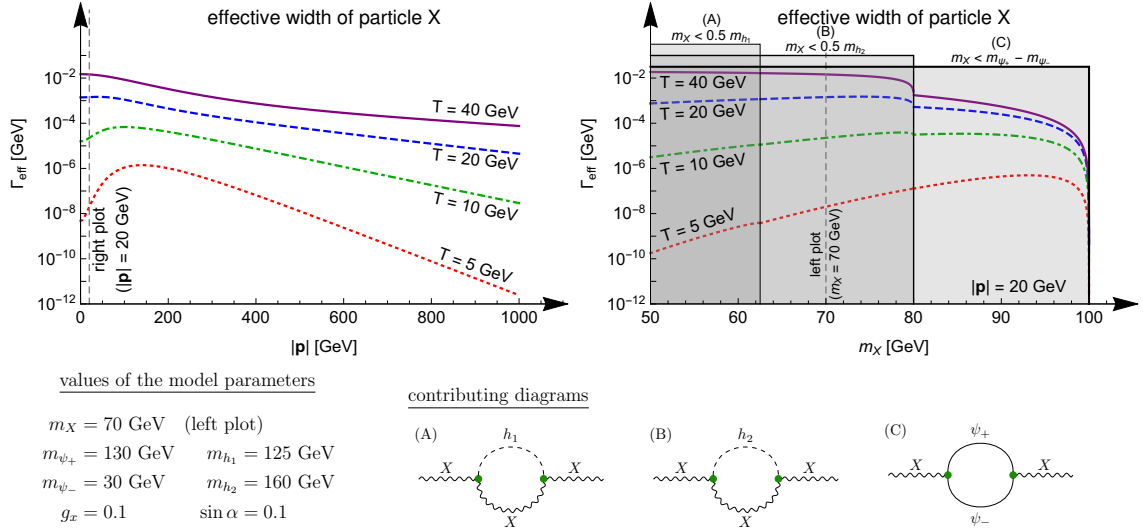


Figure 5. Effective width of particle X , acquired as a result of interactions with a thermal medium of temperature $T = 5 \text{ GeV}$ (dotted red), $T = 10 \text{ GeV}$ (dot-dashed green), $T = 20 \text{ GeV}$ (dashed blue), and $T = 40 \text{ GeV}$ (solid purple), plotted as a function of particle's momentum $|\mathbf{p}|$ (**left**) and particle's mass m_X (**right**). In each plot, the dashed vertical line indicates the value of the parameter corresponding to the other plot. In the **right** plot, each gray rectangle (A), (B), (C) corresponds to the range of m_x for which a given loop (shown in the diagrams below the plots) contributes to the effective width. Used values of the model parameters are provided below the plots.

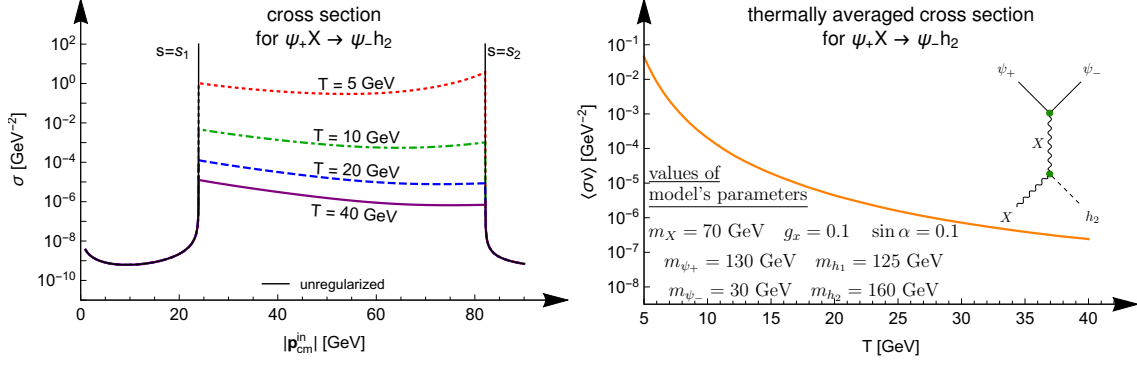


Figure 6. **Left:** regularized cross section for the $\psi_+ X \leftrightarrow \psi_- h_2$ process plotted as a function of initial state CM momentum $|\mathbf{p}_{\text{cm}}^{\text{in}}|$. The solid black line corresponds to the unregularized result (which is singular between $s = s_1$ and $s = s_2$), while the other lines show the regularized result for temperature of the medium equal to $T = 5$ GeV (dotted red), $T = 10$ GeV (dot-dashed green), $T = 20$ GeV (dashed blue), and $T = 40$ GeV (solid purple). Apparent non-smoothness of the coloured lines at $s = s_{1,2}$ is just an effect of used scale. **Right:** Regularized thermally averaged cross section for the $\psi_+ X \leftrightarrow \psi_- h_2$ process as a function of temperature of the medium T . Used values of model parameters (the same as in fig. 5) and a diagram of the considered process are provided.

Similarly, the plots provided in fig. 7 show the values of Γ_{eff} calculated for particle ψ_+ being the mediator. Figure 8 shows the cross section and the thermally averaged cross section calculated for the singular process $X\psi_+ \rightarrow \psi_- h_2$ mediated by a t -channel ψ_+ , regularized by the effective width shown in fig. 5.

Figures 7 and 8 are, in some sense, symmetric to figs. 5 and 6. The difference is that the masses of particles X and ψ_+ used to prepare the second set are swapped with respect to the first one, making it possible to compare processes of the same kinematics, but different spin of the mediating particle: $1/2$ for figs. 7 and 8, 1 for figs. 5 and 6.

Note that, in the notation assumed here, the processes denoted $\psi_+ X \rightarrow \psi_- h_2$ and $X\psi_+ \rightarrow \psi_- h_2$, although sharing the same initial and final states, are given by two different diagrams shown in figs. 6 and 8, respectively. For the first of them, it is necessary for the singularity to occur that $m_{\psi_+} > m_X + m_{\psi_-}$, while for the second one, $m_X > m_{\psi_+} + m_{\psi_-}$ must hold.

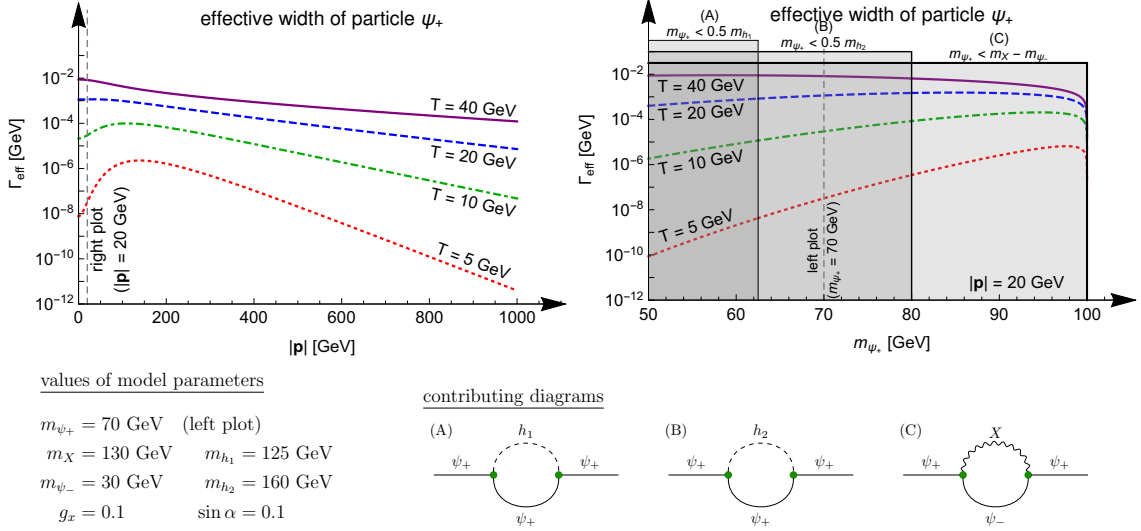


Figure 7. Effective width of particle ψ_+ , acquired as a result of interactions with a thermal medium of temperature $T = 5 \text{ GeV}$ (dotted red), $T = 10 \text{ GeV}$ (dot-dashed green), $T = 20 \text{ GeV}$ (dashed blue), and $T = 40 \text{ GeV}$ (solid purple), plotted as a function of particle's momentum $|\mathbf{p}|$ (**left**) and particle's mass m_{ψ_+} (**right**). In each plot, the dashed vertical line indicate the value of the parameter corresponding to the other plot. In the **right** plot, each gray rectangle (A), (B), (C) corresponds to the range of m_{ψ_+} for which a given loop (shown in the diagrams below the plots) contributes to the effective width. Used values of model parameters are provided below the plots.

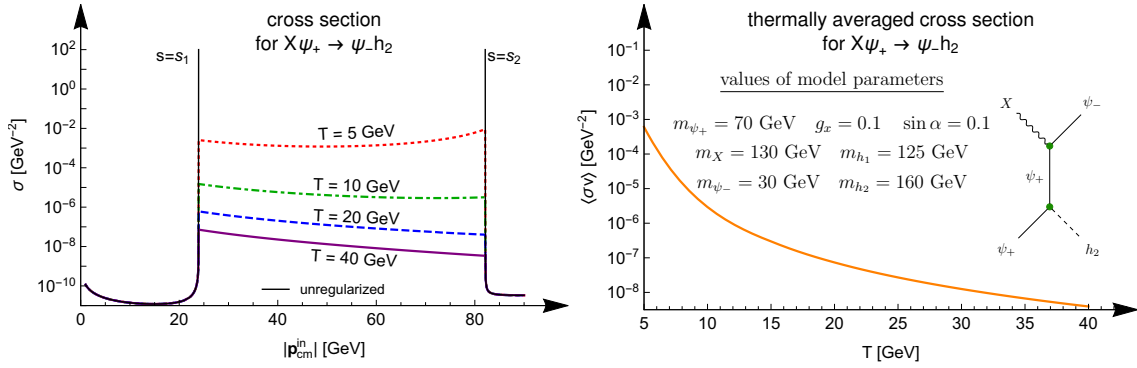


Figure 8. **Left:** regularized cross section for the $X\psi_+ \leftrightarrow \psi_-h_2$ process plotted as a function of initial state CM momentum $|\mathbf{p}_{\text{cm}}^{\text{in}}|$. The solid black line corresponds to the unregularized result (which is singular between $s = s_1$ and $s = s_2$), while the other lines show the regularized result for temperature of the medium equal to $T = 5 \text{ GeV}$ (dotted red), $T = 10 \text{ GeV}$ (dot-dashed green), $T = 20 \text{ GeV}$ (dashed blue), and $T = 40 \text{ GeV}$ (solid purple). Apparent non-smoothness of the coloured lines at $s = s_{1,2}$ is just an effect of used scale. **Right:** Regularized thermally averaged cross section for the $X\psi_+ \leftrightarrow \psi_-h_2$ process as a function of temperature of the medium T . Used values of model parameters (the same as in fig. 7) and a diagram of the considered process are provided.

5 Summary

In this paper, the method of regularization of the t -channel singularity for processes occurring in a thermal medium, presented in [16], has been generalized to the case of particles of arbitrary spins (scalars, fermions and vectors). In section 3 an analytical result for each spin case is provided.

The singularity, which would lead to infinite cross section of the processes affected, is cured by introducing an effective thermal width of the mediator. That width prevents the resummed propagator from being singular. Physically, the singularity, corresponding to would-be infinite lifetime (equivalently: free path) of the on-shell mediator, does not occur in a thermal medium because interactions between the mediator and the surrounding particles provide a channel for the mediator to vanish, making its lifetime (free path) finite.

The results presented in this paper appear to behave in a natural, expected way: the effective thermal width vanishes for small temperatures (in the limit equivalent to lack of the medium) while in finite temperature it is non-trivial even for zero mediator's momentum, see section 3.1.

To illustrate the method in action, theoretical and numerical results calculated within the Vector-Fermion Dark Matter model [17] have been presented in section 4. The plots that are shown in that section follow the behaviour predicted in section 3.1.

It is worth to stress that this work shows the full derivation of the method and demonstrates an application to an actual, specific case. This makes the presented results easy to reproduce and adapt to reader's own research.

Acknowledgements

I am grateful to B. Grzadkowski for encouraging me to write this paper and for discussions concerning it. I would also like to thank Károly Sella for a fruitful discussion and bringing my attention to the papers [13–15]. I thank St. Mrówczyński for enabling me to familiarize myself with [19].

This work has been partially supported by the National Science Centre (Poland) under grants 2017/25/B/ST2/00191 and 2020/37/B/ST2/02746.

A Conventions

This paper assumes the „mostly plus” metric tensor:

$$g_{\mu\nu} = \text{diag}(+, -, -, -) . \tag{A.1}$$

Feynman diagrams are calculated in the unitary gauge. The Feynman propagator of a scalar, a fermion and a vector particle, respectively, is given by

$$\begin{aligned}
\text{---} \overset{p}{\text{---}} \text{---} &\rightarrow i \Delta(p) \equiv \frac{i}{p^2 - m^2} , \\
\text{---} \overset{p}{\text{---}} &\rightarrow i G(p) \equiv \frac{i}{p^2 - m^2} (\not{p} + m) , \\
\mu \text{---} \overset{p}{\text{---}} \nu &\rightarrow i D_{\mu\nu}(p) \equiv \frac{i}{p^2 - m^2} \left(-g_{\mu\nu} + \frac{p_\mu p_\nu}{m^2} \right) .
\end{aligned} \tag{A.2}$$

B Green's functions

Here, following [18], the retarded (,,+"), advanced (,,−"), and symmetric (,,sym") propagators of a scalar, fermion, and vector particle are provided. For a scalar particle, in the position space, those propagators are related to the real-time Green functions $\Delta^>$, $\Delta^<$ in the following way:

$$\begin{aligned}
\Delta^{\text{sym}}(x, y) &= \Delta^>(x, y) + \Delta^<(x, y) \\
\Delta^+(x, y) &= \Theta(x_0 - y_0) (\Delta^>(x, y) - \Delta^<(x, y)) \\
\Delta^-(x, y) &= \Theta(y_0 - x_0) (\Delta^<(x, y) - \Delta^>(x, y)) ,
\end{aligned} \tag{B.1}$$

where $\Theta(t - t')$ is equal to 1 if t succeeds t' along the integration contour of the Keldysh-Schwinger formalism, -1 otherwise. Analogous relations hold for fermion and vector propagators. Details can be found in, e.g., section 4.1 of [25].

The propagators will be expressed in terms of the auxiliary functions Δ_{aux}^\pm , $\Delta_{\text{F,B}}^{\text{sym}}(p, T)$:

$$\begin{aligned}
\Delta_{\text{aux}}^\pm(p) &\equiv \frac{1}{p^2 - m^2 \pm i \text{sgn} p_0 0^+} , \\
\Delta_{\text{F,B}}^{\text{sym}}(p, T) &\equiv \pm \frac{i\pi}{E_p} \left(\delta(E_p - p_0) [2n_{\text{F,B}}(\mathbf{p}, T) \mp 1] + \delta(E_p + p_0) [2n_{\text{F,B}}(-\mathbf{p}, T) \mp 1] \right) ,
\end{aligned} \tag{B.2}$$

where $n_{\text{F,B}}$ denotes the momentum-space distribution function of the considered kind of particles, with index F standing for fermions and B for bosons. Since in equilibrium⁸

$$n_{\text{F,B}}(-\mathbf{p}, T) = n_{\text{F,B}}(\mathbf{p}, T) = \frac{1}{e^{\beta E_p} \pm 1} , \tag{B.3}$$

the $\Delta_{\text{F,B}}^{\text{sym}}$ propagator is given by

$$\begin{aligned}
\Delta_{\text{F,B}}^{\text{sym}}(p, T) &\equiv \pm \frac{i\pi}{E_p} \left(\delta(E_p - p_0) + \delta(E_p + p_0) \right) [2n_{\text{F,B}}(\mathbf{p}, T) \mp 1] \\
&= -\frac{i\pi}{E_p} \left(\delta(E_p - p_0) + \delta(E_p + p_0) \right) \cdot f_{\text{F,B}}(\beta E_p) ,
\end{aligned} \tag{B.4}$$

⁸The assumption of equilibrium is convenient but not necessary, see footnote 1.

where

$$f_{\text{F,B}}(x) \equiv \begin{cases} \frac{e^x - 1}{e^x + 1} & \text{for fermions} \\ \frac{e^x + 1}{e^x - 1} & \text{for bosons} \end{cases} . \quad (\text{B.5})$$

For a scalar field, the retarded, advanced, and symmetric propagators are given by

$$\begin{aligned} \Delta^\pm(p) &= \Delta_{\text{aux}}^\pm(p), \\ \Delta^{\text{sym}}(p, T) &= \Delta_B^{\text{sym}}(p, T) , \end{aligned} \quad (\text{B.6})$$

while for a fermion

$$\begin{aligned} G^\pm(p) &= (\not{p} + m) \Delta_{\text{aux}}^\pm(p) , \\ G^{\text{sym}}(p, T) &= (\not{p} + m) \Delta_F^{\text{sym}}(p, T) , \end{aligned} \quad (\text{B.7})$$

and for a vector

$$\begin{aligned} D_{\mu\nu}^\pm(p) &= \left[-g_{\mu\nu} + \frac{p_\mu p_\nu}{m^2} \right] \Delta_{\text{aux}}^\pm(p) , \\ D_{\mu\nu}^{\text{sym}}(p, T) &= \left[-g_{\mu\nu} + \frac{p_\mu p_\nu}{m^2} \right] \Delta_B^{\text{sym}}(p, T) . \end{aligned} \quad (\text{B.8})$$

C Allowed range of $E_{1,2}$

In this appendix, a proof of correctness of the transition between eq. (3.14) and eq. (3.18) is presented. Let us recall the definitions of $\cos \alpha_1$, $\cos \beta_1$, $\cos \alpha_2$, and $\cos \beta_2$ given by eq. (3.15):

$$\begin{aligned} \cos \alpha_1 &\equiv \frac{-(m_1^2 - m_2^2 + M^2) + 2E_1 E_p}{2|\mathbf{k}||\mathbf{p}|} , & \cos \beta_1 &\equiv \frac{-(m_1^2 - m_2^2 + M^2) - 2E_1 E_p}{2|\mathbf{k}||\mathbf{p}|} , \\ \cos \alpha_2 &\equiv \frac{-(m_1^2 - m_2^2 - M^2) + 2E_2 E_p}{2|\mathbf{k}||\mathbf{p}|} , & \cos \beta_2 &\equiv \frac{-(m_1^2 - m_2^2 - M^2) - 2E_2 E_p}{2|\mathbf{k}||\mathbf{p}|} . \end{aligned} \quad (\text{C.1})$$

If $m_2 > |m_1 - M|$, then $\cos \alpha_1 > 1$. Indeed,

$$\cos \alpha_1 = \frac{-m_1^2 + m_2^2 - M^2 + 2E_1 E_p}{2|\mathbf{k}||\mathbf{p}|} > \frac{-2m_1 M + 2E_1 E_p}{2|\mathbf{k}||\mathbf{p}|} > 1 , \quad (\text{C.2})$$

Analogously, if $m_1 > |m_2 - M|$, then $\cos \beta_2 < -1$, since

$$\cos \beta_2 = -\frac{m_1^2 - m_2^2 - M^2 + 2E_2 E_p}{2|\mathbf{k}||\mathbf{p}|} < -\frac{-2m_2 M + 2E_2 E_p}{2|\mathbf{k}||\mathbf{p}|} < -1 . \quad (\text{C.3})$$

Moreover, if $m_2 < m_1 + M$, then $\cos \beta_1 < -1$:

$$\cos \beta_1 = -\frac{m_1^2 - m_2^2 + M^2 + 2E_1 E_p}{2|\mathbf{k}||\mathbf{p}|} < -\frac{-2m_1 M + 2E_1 E_p}{2|\mathbf{k}||\mathbf{p}|} < -1 . \quad (\text{C.4})$$

Finally, if $m_1 < m_2 + M$, then $\cos \alpha_2 > 1$:

$$\cos \alpha_2 = \frac{-m_1^2 + m_2^2 + M^2 + 2E_2 E_p}{2|\mathbf{k}||\mathbf{p}|} > \frac{-2m_2 M + 2E_2 E_p}{2|\mathbf{k}||\mathbf{p}|} > 1 , \quad (\text{C.5})$$

Together, these four statements mean that if m_1 , m_2 and M satisfy the triangle inequality, all four trigonometric functions are outside the $[-1, 1]$ interval. Therefore, for the result of eq. (3.14) to be non-zero, one of the masses must be greater than the two others. Due to the assumption of stability of the mediator, M cannot be greater than the sum of m_1 and m_2 (see ineq. (3.3)). This means that only the loops with one internal state allowed to decay into the other one and the mediator provide a non-zero contribution to the regulator.⁹ Without loss of generality it can be, therefore, assumed that

$$m_1 > m_2 + M , \quad (\text{C.6})$$

so that $\cos \beta_1$ and $\cos \beta_2$ are outside the $[-1, 1]$ interval and the delta functions containing them vanish.

Concerning the delta function containing $\cos \alpha_1$, it limits possible values of E_1 to those satisfying $|\cos \alpha_1| < 1$. It appears that

$$k^2 p^2 (\cos^2 \alpha_1 - 1) = M^2 E_1^2 - (m_1^2 - m_2^2 + M^2) E_p E_1 + m_1^2 E_p^2 + \frac{\lambda(m_1^2, m_2^2, M^2)}{4} , \quad (\text{C.7})$$

where λ denotes the so-called Källén function, defined as

$$\begin{aligned} \lambda(m_1^2, m_2^2, M^2) &\equiv m_1^4 + m_2^4 + M^4 - 2 m_1^2 m_2^2 - 2 m_1^2 M^2 - 2 m_2^2 M^2 \\ &= [m_1^2 - (m_2 - M)^2] [m_1^2 - (m_2 + M)^2] . \end{aligned} \quad (\text{C.8})$$

E_1 is in the allowed range if the quantity (C.7) is negative, which can be reduced to the following condition:

$$b - a < E_1 < b + a , \quad (\text{C.9})$$

where

$$b \equiv \frac{m_1^2 - m_2^2 + M^2}{2M^2} E_p , \quad a \equiv \frac{\lambda(m_1^2, m_2^2, M^2)^{1/2}}{2M^2} |\mathbf{p}| . \quad (\text{C.10})$$

Analogously, it can be shown that the delta function containing $\cos \alpha_2$ limits the range of E_2 to

$$b - a - E_p < E_2 < b + a - E_p . \quad (\text{C.11})$$

Note that

$$b - a - E_p = \frac{m_1^2 - m_2^2 - M^2}{2M^2} E_p - \frac{\lambda(m_1^2, m_2^2, M^2)^{1/2}}{2M^2} |\mathbf{p}| \quad (\text{C.12})$$

is positive since

$$m_1^2 - m_2^2 - M^2 > \sqrt{(m_1^2 - m_2^2 - M^2)^2 - 4 m_2^2 M^2} = \lambda(m_1^2, m_2^2, M^2)^{1/2} \quad (\text{C.13})$$

and

$$E_p > |\mathbf{p}| . \quad (\text{C.14})$$

⁹Such a loop always exists because for the considered t -channel process to be singular it is necessary that the mediator can be produced in a decay process, see condition (1.1). Consequently, any t -channel singular $2 \rightarrow 2$ process occurring in a medium can be regularized using the method described in this paper.

D Calculation of X_0 in the general case

Here, the factor X_0 is calculated for all loops that can be generated using particles of spin 0, 1/2 and 1. Tables 4 to 6 show the results for the case of a scalar, a fermion and a vector mediator, respectively.

| loop | relevant vertex | spin & vertex factor | $X_0 \equiv [\text{spin \& vertex factor}]_{\text{on-shell}}$ |
|------|-----------------|--|---|
| | | $-\mu^2$ | $-\mu^2$ |
| | | $-g^2(p_1 + p)^\alpha(p_1 + p)^\beta \left(-g_{\alpha\beta} + \frac{p_{2\alpha}p_{2\beta}}{m_2^2} \right)$ | $-g^2 \frac{\lambda(m_1^2, m_2^2, M^2)}{m_2^2}$ |
| | | $-g^2(p_2 - p)^\alpha(p_2 - p)^\beta \left(-g_{\alpha\beta} + \frac{p_{1\alpha}p_{1\beta}}{m_1^2} \right)$ | $-g^2 \frac{\lambda(m_1^2, m_2^2, M^2)}{m_1^2}$ |
| | | $-\mu^2 \left(-g_{\alpha\beta} + \frac{p_{1\alpha}p_{1\beta}}{m_1^2} \right) \left(-g^{\alpha\beta} + \frac{p_{2\alpha}p_{2\beta}}{m_2^2} \right)$ | $-\mu^2 \left[\frac{\lambda(m_1^2, m_2^2, M^2)}{4m_1^2 m_2^2} + 3 \right]$ |
| | | $-(-1)\text{Tr} \left[(Y_v^* + i Y_a^* \gamma_5)(p_1 + m_1) \times (Y_v + i Y_a \gamma_5)(p_2 + m_2) \right]$ | $2 Y_v ^2 [(m_1 + m_2)^2 - M^2] + 2 Y_a ^2 [(m_1 - m_2)^2 - M^2]$ |

Table 4. Factor X_0 calculated for all loops relevant in the case of a scalar mediator. In the third column, „spin & vertex factor” denotes the matrix element corresponding to the loop, multiplied by $(-i)^2 [p_1^2 - m_1^2] [p_2^2 - m_2^2]$, before integration over loop momenta. In the fourth column, the factor X_0 is calculated assuming that all particles are on-mass-shell. Note that X_0 is always positive (negative) for particle „2” being a fermion (boson) given that $m_1 > m_2 + M$. Scalar and vector states are assumed to be real (not complex). Here, g is real and dimensionless, μ is real and has dimension of mass, while Y_v and Y_a are complex and dimensionless.

| loop | relevant vertex | spin & vertex factor | $X_0 \equiv \frac{1}{2} \text{Tr} [(\not{p} + M) [\text{spin \& vertex f.}]]_{\text{on-shell}}$ |
|------|-----------------|--|--|
| | | $-(Y_v^* + i Y_a^* \gamma_5)(-\not{p}_2 + m_2)(Y_v + i Y_a \gamma_5)$ | $\frac{ Y_v ^2}{2} [m_1^2 - (m_2 + M)^2] + \frac{ Y_a ^2}{2} [m_1^2 - (m_2 - M)^2]$ |
| | | $-(Y_v^* + i Y_a^* \gamma_5)(\not{p}_1 + m_1)(Y_v + i Y_a \gamma_5)$ | $-\frac{ Y_v ^2}{2} [(m_1 + M)^2 - m_2^2] - \frac{ Y_a ^2}{2} [(m_1 - M)^2 - m_2^2]$ |
| | | $-\gamma^\beta (G_v^* + G_a^* \gamma_5)(-\not{p}_2 + m_2) \gamma^\alpha (G_v + G_a \gamma_5) \left(-g_{\alpha\beta} + \frac{p_{1\alpha} p_{1\beta}}{m_1^2} \right)$ | $\frac{ G_v ^2}{2} [2m_1^2 + (m_2 + M)^2] \frac{m_1^2}{m_1^2} \frac{[m_1^2 - (m_2 - M)^2]}{m_1^2} + \frac{ G_a ^2}{2} [2m_1^2 + (m_2 - M)^2] \frac{m_1^2}{m_1^2} \frac{[m_1^2 - (m_2 + M)^2]}{m_1^2}$ |
| | | $-\gamma^\beta (G_v^* + G_a^* \gamma_5)(\not{p}_1 + m_1) \gamma^\alpha (G_v + G_a \gamma_5) \left(-g_{\alpha\beta} + \frac{p_{2\alpha} p_{2\beta}}{m_2^2} \right)$ | $-\frac{ G_v ^2}{2} [(m_1 + M)^2 + 2m_2^2] \frac{m_2^2}{m_2^2} \frac{[(m_1 - M)^2 - m_2^2]}{m_2^2} - \frac{ G_a ^2}{2} [(m_1 - M)^2 + 2m_2^2] \frac{m_2^2}{m_2^2} \frac{[(m_1 + M)^2 - m_2^2]}{m_2^2}$ |

Table 5. Like table 4, but for a fermion mediator. Here, Y_v , Y_a , G_v , and G_a are complex and dimensionless.

| loop | relevant vertex | spin & vertex factor | $X_0 \equiv \frac{1}{3} \left[\left(-g_{\alpha\beta} + \frac{p_{1\alpha} p_{1\beta}}{m_1^2} \right) \times [\text{spin \& vertex f.}]^{\alpha\beta} \right]_{\text{on-shell}}$ |
|------|-----------------|---|--|
| | | $-g^2 (p_1 + p_2)^\alpha (p_1 + p_2)^\beta$ | $-\frac{g^2}{3} \frac{\lambda(m_1^2, m_2^2, M^2)}{M^2}$ |
| | | $-\mu^2 \left(-g^{\alpha\beta} + \frac{p_{2\alpha} p_{2\beta}}{m_2^2} \right)$ | $-\frac{\mu^2}{3} \left[\frac{\lambda(m_1^2, m_2^2, M^2)}{4m_2^2 M^2} + 3 \right]$ |
| | | $-\mu^2 \left(-g^{\alpha\beta} + \frac{p_{1\alpha} p_{1\beta}}{m_1^2} \right)$ | $-\frac{\mu^2}{3} \left[\frac{\lambda(m_1^2, m_2^2, M^2)}{4m_1^2 M^2} + 3 \right]$ |
| | | $-f_{ABC}^2 \left(-g_{\mu\nu} + \frac{p_{1\mu} p_{1\nu}}{m_1^2} \right) \left(-g_{\rho\sigma} + \frac{p_{2\rho} p_{2\sigma}}{m_2^2} \right) \times [g^{\nu\sigma} (p_1 + p_2)^\beta + g^{\sigma\beta} (p - p_2)^\nu - g^{\beta\nu} (p + p_1)^\sigma] \times [g^{\mu\rho} (p_1 + p_2)^\alpha + g^{\rho\alpha} (p - p_2)^\mu - g^{\alpha\mu} (p + p_1)^\rho]$ | $-\frac{f_{ABC}^2}{3} \frac{g_{\mu\nu} \lambda(m_1^2, m_2^2, M^2)}{4m_1^2 m_2^2 M^2} \times \frac{\lambda(m_1^2, m_2^2, M^2) + 12(m_1^2 M^2 + m_2^2 M^2 + m_1^2 m_2^2)}{4m_1^2 m_2^2 M^2}$ |
| | | $-(-1) \text{Tr} [\gamma^\beta (G_v^* + G_a^* \gamma_5)(\not{p}_1 + m_1) \gamma^\alpha (G_v + G_a \gamma_5)(\not{p}_2 + m_2)]$ | $\frac{2}{3} G_v ^2 \frac{[(m_1 - m_2)^2 - M^2]}{M^2} \frac{[(m_1 + m_2)^2 + 2M^2]}{M^2} + \frac{2}{3} G_a ^2 \frac{[(m_1 + m_2)^2 - M^2]}{M^2} \frac{[(m_1 - m_2)^2 + 2M^2]}{M^2}$ |

Table 6. Like table 4, but for a vector mediator. Here, g and f_{klm} are real and dimensionless, μ is real and has dimension of mass, while G_v and G_a are complex and dimensionless. It is assumed that f_{klm} is totally antisymmetric in its indices.

E Calculation of X_0 within the VFDM model

In this appendix, the values of the factor X_0 calculated for dark mediators present in the VFDM model (see section 4) are presented. Figure 9 shows the relevant vertices while fig. 10 provides the spin-dependent factors needed to calculate X_0 . Tables 7 to 9 present the values of X_0 for all contributing loops, basing on the results of appendix D.

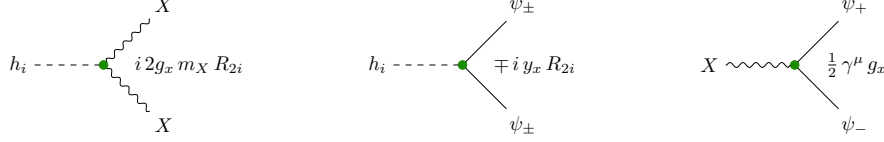


Figure 9. Relevant vertices of the VFDM model and their values.

$$\begin{aligned}
 \text{---} \frac{p}{h_i} \text{---} &\rightarrow 1 & \mu \sim \frac{p}{X} \nu &\rightarrow -g_{\mu\nu} + \frac{p_\mu p_\nu}{m_X^2} & \frac{p}{\psi_\pm} &\rightarrow \not{p} + m_{\psi_\pm}
 \end{aligned}$$

Figure 10. Spin factors (i.e., propagators with the factor $i [p^2 - m^2 \pm i 0^+]^{-1}$ omitted) corresponding to the relevant particles of the model.

| loop | vertex | X_0 | $X_0 / \mathcal{M} _{i \rightarrow M2}^2$ | condition |
|------|--------|---|--|---------------------------------|
| | | $\frac{1}{6} g_x^2 \frac{[(m_{\psi_+} - m_{\psi_-})^2 - m_X^2][(m_{\psi_+} + m_{\psi_-})^2 + 2m_X^2]}{m_X^2}$ | $\frac{1}{3}$ | $m_{\psi_+} > m_X + m_{\psi_-}$ |
| | | $-\frac{1}{3} g_x^2 R_{2i}^2 \frac{m_{h_i}^4 - 4 m_{h_i}^2 m_X^2 + 12 m_X^4}{m_X^2}$ | $-\frac{1}{3}$ | $m_{h_i} > 2 m_X$ |

Table 7. Factor X_0 calculated within the VFDM model for particle X being the mediator. The last but one column contains the ratio between X_0 and the matrix-element-squared corresponding to the decay of the upper loop state into the lower loop state and the mediator (symbols „1”, „2” and „M” correspond to those in fig. 4). The last column presents the condition for the given loop to contribute to the mediator’s thermal width.

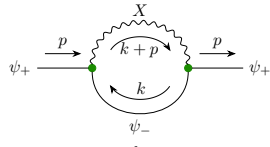
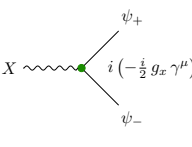
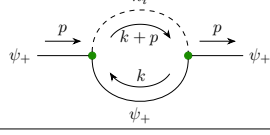
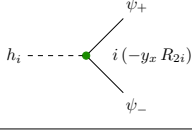
| loop | vertex | X_0 | $X_0 / \mathcal{M} _{1 \rightarrow M2}^2$ | condition |
|---|---|--|--|---|
|  |  | $i \left(-\frac{i}{2} g_x \gamma^\mu \right)$ | $\frac{1}{4} g_x^2 \frac{[m_X^2 - (m_{\psi_+} - m_{\psi_-})^2] [2m_X^2 + (m_{\psi_+} + m_{\psi_-})^2]}{m_X^4}$ | $\frac{1}{2} \quad m_X > m_{\psi_+} + m_{\psi_-}$ |
|  |  | $i (-y_x R_{2i})$ | $y_x^2 R_{2i}^2 (m_{h_i}^2 - 4m_{\psi_+}^2)$ | $\frac{1}{2} \quad m_{h_i} > 2m_{\psi_+}$ |

Table 8. Like table 1, but for particle ψ_+ being the mediator.

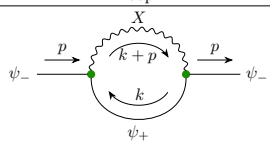
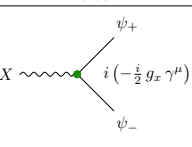
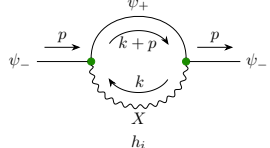
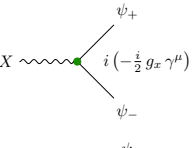
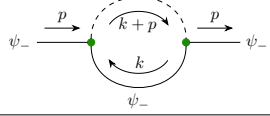
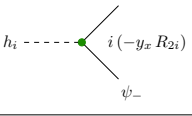
| loop | vertex | X_0 | $X_0 / \mathcal{M} _{1 \rightarrow M2}^2$ | condition |
|---|---|--|---|--|
|  |  | $i \left(-\frac{i}{2} g_x \gamma^\mu \right)$ | $\frac{1}{4} g_x^2 \frac{[m_X^2 - (m_{\psi_+} - m_{\psi_-})^2] [2m_X^2 + (m_{\psi_+} + m_{\psi_-})^2]}{m_X^4}$ | $\frac{1}{2} \quad m_X > m_{\psi_+} + m_{\psi_-}$ |
|  |  | $i \left(-\frac{i}{2} g_x \gamma^\mu \right)$ | $-\frac{1}{4} g_x^2 \frac{[(m_{\psi_+} - m_{\psi_-})^2 - m_X^2] [(m_{\psi_+} + m_{\psi_-})^2 + 2m_X^2]}{m_X^4}$ | $-\frac{1}{2} \quad m_{\psi_+} > m_X + m_{\psi_-}$ |
|  |  | $i (-y_x R_{2i})$ | $y_x^2 R_{2i}^2 (m_{h_i}^2 - 4m_{\psi_-}^2)$ | $\frac{1}{2} \quad m_{h_i} > 2m_{\psi_-}$ |

Table 9. Like table 1, but for particle ψ_- being the mediator.

F Results of Weldon's paper

According to Weldon's paper [14], the imaginary part of thermal self-energy corresponding to a loop consisting of particles „1” and „2” (see fig. 4) can be expressed as:

$$\Sigma = \frac{1}{2} \int \frac{d^3 p_1}{(2\pi)^3 2E_1} \frac{d^3 p_2}{(2\pi)^3 2E_2} (2\pi)^4 \delta^{(4)}(p_1 - p_2 - p) |\mathcal{M}_{1 \rightarrow 2, M}|^2 [\eta n_1(\beta E_1) + n_2(\beta E_2)] , \quad (\text{F.1})$$

where

$$\eta \equiv \begin{cases} -1 & \text{if particles 1 and 2 are both bosons (both fermions)} \\ +1 & \text{otherwise} \end{cases} , \quad (\text{F.2})$$

while $n_i(x) \equiv (e^x \pm 1)^{-1}$, $i = 1, 2$ is the thermal distribution function, with the \pm sign being a plus if particle i is a fermion and a minus for a boson. After integration over $d^3 p_2$

and a change of variables, the integral reads

$$\Sigma = \frac{1}{16\pi|\mathbf{p}|} \int_{m_1}^{\infty} dE_1 \int_{-1}^1 d\cos\theta \delta(\cos\theta - \cos\theta_0) |\mathcal{M}_{1\rightarrow 2,M}|^2 [\eta n_1(\beta E_1) + n_2(\beta E_2)] , \quad (\text{F.3})$$

where

$$\cos\theta_0(E_1) \equiv \frac{2E_p E_1 - (m_1^2 - m_2^2 + M^2)}{2|\mathbf{p}||\mathbf{p}_1|} \quad (\text{F.4})$$

is the value of $\cos\theta$ (θ denotes the angle between \mathbf{p} and \mathbf{p}_1) corresponding to $E_1 = E_2 + E_p$. The delta function limits the range of integration over E_1 to the values giving $|\cos\theta_0| < 1$:

$$\Sigma = \frac{1}{16\pi|\mathbf{p}|} \int_{E_-}^{E_+} dE_1 |\mathcal{M}_{1\rightarrow 2,M}|^2 [\eta n_1(\beta E_1) + n_2(\beta E_1 - \beta E_p)] , \quad (\text{F.5})$$

where

$$E_{\pm} \equiv b \pm a , \quad a \equiv \frac{|\mathbf{p}| \sqrt{\lambda(m_1^2, m_2^2, M^2)}}{2M^2} , \quad b \equiv \frac{m_1^2 - m_2^2 + M^2}{2M^2} E_p , \quad (\text{F.6})$$

$$\lambda(m_1^2, m_2^2, M^2) \equiv [m_1^2 - (m_2 - M)^2] [m_1^2 - (m_2 + M)^2] .$$

Then, assuming Lorentz invariance of $|\mathcal{M}_{1\rightarrow 2,M}|^2$, the result can be transformed to

$$\begin{aligned} \Sigma &= \Sigma(E_p, T) = \frac{|\mathcal{M}_{1\rightarrow 2,M}|^2}{16\pi|\mathbf{p}|} \int_{E_-}^{E_+} dE_1 [\eta n_1(\beta E_1) + n_2(\beta E_1 - \beta E_p)] \\ &= \frac{|\mathcal{M}_{1\rightarrow 2,M}|^2}{16\pi\beta|\mathbf{p}|} \left[\eta \int_{\beta E_-}^{\beta E_+} n_1(x) dx + \int_{\beta(E_- - E_p)}^{\beta(E_+ - E_p)} n_2(x) dx \right] \end{aligned} \quad (\text{F.7})$$

After integration, this becomes

$$\Sigma(E_p, T) = \frac{1}{16\pi} \frac{|\mathcal{M}_{1\rightarrow 2,M}|^2}{\beta|\mathbf{p}|} \left[\ln \frac{e^{\beta(b+a)} + \eta_1}{e^{\beta(b-a)} + \eta_1} - \ln \frac{e^{\beta(b+a)} e^{-\beta E_p} + \eta_2}{e^{\beta(b-a)} e^{-\beta E_p} + \eta_2} \right] , \quad (\text{F.8})$$

where

$$\begin{aligned} \eta_i &\equiv \begin{cases} -1 & \text{particle } i \text{ is a boson} \\ +1 & \text{particle } i \text{ is a fermion} \end{cases} , \\ a &\equiv \frac{|\mathbf{p}| \sqrt{\lambda(m_1^2, m_2^2, M^2)}}{2M^2} , \quad b \equiv \frac{m_1^2 - m_2^2 + M^2}{2M^2} E_p , \\ \lambda(m_1^2, m_2^2, M^2) &\equiv [m_1^2 - (m_2 - M)^2] [m_1^2 - (m_2 + M)^2] , \\ \beta &\equiv \frac{1}{T} , \quad |\mathbf{p}| \equiv \sqrt{E_p^2 - M^2} . \end{aligned} \quad (\text{F.9})$$

This result differs slightly from eq. (3.23) with X_0 provided in appendix E, namely, it lacks the factor of $1/2$ or $1/3$ for a fermion or vector mediator, respectively.

References

- [1] R.F. Peierls, *Possible Mechanism for the Pion-Nucleon Second Resonance*, *Phys. Rev. Lett.* **6** (1961) 641.
- [2] S. Coleman and R.E. Norton, *Singularities in the physical region*, *Nuovo Cim.* **38** (1965) 438.
- [3] D.D. Brayshaw, W.A. Simmons and S.F. Tuan, *Some comments on the Brayshaw mechanism for generating peaks in the hadron system*, *Phys. Rev. D* **18** (1978) 1719.
- [4] I.F. Ginzburg, *Initial particle instability in muon collisions*, *Nucl. Phys. B Proc. Suppl.* **51** (1996) 85 [[hep-ph/9601272](#)].
- [5] K. Melnikov and V.G. Serbo, *New type of beam size effect and the W boson production at $\mu\mu$ colliders*, *Phys. Rev. Lett.* **76** (1996) 3263 [[hep-ph/9601221](#)].
- [6] K. Melnikov and V.G. Serbo, *Processes with the T channel singularity in the physical region: Finite beam sizes make cross-sections finite*, *Nucl. Phys. B* **483** (1997) 67 [[hep-ph/9601290](#)].
- [7] K. Melnikov, G.L. Kotkin and V.G. Serbo, *Physical mechanism of the linear beam size effect at colliders*, *Phys. Rev. D* **54** (1996) 3289 [[hep-ph/9603352](#)].
- [8] C. Dams and R. Kleiss, *Singular cross-sections in muon colliders*, *Eur. Phys. J. C* **29** (2003) 11 [[hep-ph/0212301](#)].
- [9] C. Dams and R. Kleiss, *Muon colliders, Monte Carlo and gauge invariance*, *Eur. Phys. J. C* **36** (2004) 177 [[hep-ph/0309336](#)].
- [10] A. Ioannisian and A. Pilaftsis, *Neutrino oscillations in space within a solvable model*, *Phys. Rev. D* **59** (1999) 053003 [[hep-ph/9809503](#)].
- [11] D. Karamitros and A. Pilaftsis, *Towards a Non-Local S -Matrix Theory*, [2208.10425](#).
- [12] E. Braaten and R.D. Pisarski, *Soft Amplitudes in Hot Gauge Theories: A General Analysis*, *Nucl. Phys. B* **337** (1990) 569.
- [13] G.F. Giudice, A. Notari, M. Raidal, A. Riotto and A. Strumia, *Towards a complete theory of thermal leptogenesis in the SM and MSSM*, *Nucl. Phys. B* **685** (2004) 89 [[hep-ph/0310123](#)].
- [14] H.A. Weldon, *Simple Rules for Discontinuities in Finite Temperature Field Theory*, *Phys. Rev. D* **28** (1983) 2007.
- [15] D.A. Dicus, E.W. Kolb, A.M. Gleeson, E.C.G. Sudarshan, V.L. Teplitz and M.S. Turner, *Primordial Nucleosynthesis Including Radiative, Coulomb, and Finite Temperature Corrections to Weak Rates*, *Phys. Rev. D* **26** (1982) 2694.
- [16] B. Grzadkowski, M. Iglicki and S. Mrówczyński, *t -channel singularities in cosmology and particle physics*, *Nucl. Phys. B* **984** (2022) 115967 [[2108.01757](#)].
- [17] A. Ahmed, M. Duch, B. Grzadkowski and M. Iglicki, *Multi-Component Dark Matter: the vector and fermion case*, *Eur. Phys. J. C* **78** (2018) 905 [[1710.01853](#)].
- [18] A. Czajka and S. Mrowczynski, *Collective Excitations of Supersymmetric Plasma*, *Phys. Rev. D* **83** (2011) 045001 [[1011.6028](#)].
- [19] M.L. Bellac, *Thermal Field Theory*, Cambridge Monographs on Mathematical Physics, Cambridge University Press (3, 2011), [10.1017/CBO9780511721700](#).
- [20] A. Das, A. Bandyopadhyay, P.K. Roy and M.G. Mustafa, *General structure of fermion two-point function and its spectral representation in a hot magnetized medium*, *Phys. Rev. D* **97** (2018) 034024 [[1709.08365](#)].

- [21] M.O. Gonchar, A.E. Kaloshin and V.P. Lomov, *Fermion resonance in quantum field theory*, *Mod. Phys. Lett. A* **22** (2007) 2511 [[hep-ph/0611314](#)].
- [22] M. Nowakowski and A. Pilaftsis, *On gauge invariance of Breit-Wigner propagators*, *Z. Phys. C* **60** (1993) 121 [[hep-ph/9305321](#)].
- [23] L.P. Kadanoff and G. Baym, *Quantum Statistical Mechanics*, CRC Press (Mar., 2018), [10.1201/9780429493218](#).
- [24] S. Mrowczynski and P. Danielewicz, *Green Function Approach to Transport Theory of Scalar Fields*, *Nucl. Phys. B* **342** (1990) 345.
- [25] A. Czajka, *Supersymmetric plasma systems and their nonsupersymmetric counterparts*, Ph.D. thesis, Jan Kochanowski U., 2015. [1601.08215](#).